INTERNATIONAL JOURNAL OF MEDICAL SCIENCE AND DENTAL HEALTH
(ISSN: 2454-4191)
www.ijmsdh.org (2026)

Received: 10 Aug 2026
Revised: 29 Aug 2026
Accepted: 09 Sep 2026
Published: 18 Sep 2026

Volume 12 Issue 09, 2026
Page No - 161-163
DOI - 10.55640/ijmsdh-12-09-18

Article Citation: Kaymanova Kamila Imamovna, & Sanoev Baxtiyor Abdurasulovich. (2026). Immunohistochemical Expression of Ki-67 And Cd34 In the Kidney in Experimentally Induced Ulcerative Colitis: Proliferative Activity and Microvascular Remodeling in Rats. International Journal of Medical Science and Dental Health, 12(09), 155-163. https://doi.org/10.55640/ijmsdh-12-09-18

Immunohistochemical Expression of Ki-67 And Cd34 In the Kidney in Experimentally Induced Ulcerative Colitis: Proliferative Activity and Microvascular Remodeling in Rats

Kaymanova Kamila Imamovna

Department of Histology, Cytology and Embryology of Bukhara State Medical Institute Named After Abu Ali Ibn Sino, Uzbekistan

Sanoev Baxtiyor Abdurasulovich

Bukhara State Medical Institute Named After Abu Ali Ibn Sino, Department of Pathological Anatomy and Pathological Physiology, Bukhara, Uzbekistan

Abstract

Background. Ulcerative colitis (UC) is a chronic relapsing inflammatory bowel disease (IBD) with frequent extraintestinal, including renal, involvement. The behaviour of the proliferation marker Ki-67 and the endothelial/microvascular marker CD34 in the kidney under experimental UC is insufficiently characterised.

Methods. Sixty 9-month-old white outbred rats were studied: a control group (n = 20) and a UC group (n = 40; 5 deaths). UC was induced by a single intrarectal instillation of 1 mL of 8 % acetic acid followed by 20 days of observation. Paraffin kidney sections (4–5 μm) were immunostained for Ki-67 and CD34 using heat-induced epitope retrieval in citrate buffer (pH 6.0), an avidin–biotin peroxidase system and 3,3′-diaminobenzidine (DAB), with haematoxylin counterstain. CD34 microvessel density (MVD) was assessed by the Weidner hotspot method (≥ 5 fields, ×200) and the relative CD34-positive area by digital analysis (QuPath 0.5.0). Data were summarised as mean ± SD and analysed in IBM SPSS Statistics 23.

Results. In controls, renal Ki-67 nuclear staining was rare and sporadic, in keeping with the very low baseline proliferation of the normal kidney. In the UC group the Ki-67 index rose markedly (mean 35.4 %; range 22.7–59.7 %), predominantly in the tubular epithelium of injury zones, in interstitial inflammatory cells (lymphocytes, histiocytes, fibroblasts) and in glomerular mesangial cells, whereas capillary endothelium and podocytes remained negative. CD34 MVD fell

from 45.2 ± 2.1 to 32.8 vessels/mm² (−27.4 %), with peritubular capillary rarefaction in fibrotic areas, reduced glomerular CD34 accompanying mesangial expansion, and only focal neoangiogenesis; the mean CD34-positive area was 59.3 %.

Conclusion. Experimental UC produces a dissociation between enhanced cellular proliferation and microvascular rarefaction in the kidney, a combination that favours progression of interstitial fibrosis. Ki-67 and CD34 are promising quantitative markers for early detection and monitoring of UC-associated renal injury.

Keywords: Ulcerative colitis; kidney; Ki-67; CD34; microvessel density; peritubular capillary rarefaction; immunohistochemistry; experimental colitis; gut–kidney axis.

1. Introduction

Inflammatory bowel disease (IBD), comprising ulcerative colitis (UC) and Crohn's disease, is a chronic, immune-mediated, relapsing–remitting disorder of the gastrointestinal tract associated with systemic inflammation and immune dysregulation. Extraintestinal manifestations affect a large proportion of patients — up to about 47 % in contemporary series — yet kidney and urinary-tract involvement remains comparatively under-recognised [1].

Renal involvement is reported in roughly 4–23 % of patients with IBD and encompasses a wide spectrum, including nephrolithiasis, glomerular disease (particularly IgA nephropathy), tubulointerstitial nephritis, acute kidney injury, chronic kidney disease (CKD) and, more rarely, secondary (AA) amyloidosis [1–3]. Large epidemiological analyses indicate an elevated risk of CKD in IBD, with a reported ~1.59-fold increase in odds relative to non-IBD populations [1,4]. The underlying pathogenesis reflects complex gut–kidney interactions — systemic inflammation and circulating immune complexes, intestinal dysbiosis with nephrotoxic microbial metabolites, shared genetic and immune pathways, and drug-related nephrotoxicity [1,5,6].

Because the clinical renal manifestations of UC may be subtle and are difficult to study prospectively, experimental models are essential for dissecting the underlying tissue mechanisms. Intrarectal instillation of acetic acid is a widely used, reproducible model that recapitulates key features of human UC, including mucosal ulceration, oxidative stress and systemic inflammatory spill-over, and has been used to examine hepatic and renal consequences of colitis [7,8].

Two immunohistochemical (IHC) markers are particularly informative for characterising the renal response. Ki-67 is a nuclear antigen expressed in all active phases of the cell cycle and is the standard marker of proliferative activity. In the healthy kidney the Ki-67 proliferation index is very low — of the order of 0.2–0.5 % in tubular epithelium and about 0.1 % in the mesangium [9]; it rises when tubular epithelial cells re-enter the cell cycle during repair after injury and when mesangial and interstitial cells proliferate, and it has been used to gauge disease activity in IgA and lupus nephritis [9–12]. CD34 is a transmembrane glycoprotein expressed by vascular endothelium and is routinely used to visualise the renal microvasculature and to quantify microvessel density (MVD). Loss of peritubular capillaries (capillary rarefaction), reflected by falling CD34 expression, is a hallmark of progressive tubulointerstitial injury and renal fibrosis and correlates with declining renal function [13–16].

Although both markers are individually established, their combined use — together with morphometry — to characterise renal injury in experimental UC remains scarce and unsystematised. The present study therefore evaluated the immunohistochemical expression of Ki-67 and CD34 in the kidneys of rats with experimentally induced UC, in order to define the balance between cellular proliferation and microvascular remodelling and to identify candidate quantitative criteria for early renal injury.

2. Methods

2.1. Animals and study design

The study was performed on 60 sexually mature white outbred rats aged 9 months. Animals were housed under standard vivarium conditions with free access to water and standard chow and were randomly allocated to groups to ensure representativeness. All procedures complied with institutional bioethical requirements and biosafety norms and were approved by the local Ethics Committee prior to the experiment (see Ethics statement). The distribution of animals is summarised in Table 1.

Group	Experimental content	Age	Animals (deaths)
I (control)	Intact control group used for direct comparison with the experimental group	9 months	20
II (UC)	Ulcerative colitis induced by a single intrarectal instillation of 1 mL of 8 % acetic acid, followed by 20 days of observation	9 months	40 (5)
Total			60 (5)

Table 1. Distribution of animals according to the experimental design. Deaths during the observation period are given in parentheses.

2.2. Induction of experimental ulcerative colitis

Before induction, animals were fasted for a defined period with free access to water to clear the distal colon and to allow direct contact of the modelling solution with the mucosa. After gentle restraint, the tip of an atraumatic probe was lubricated with sterile petrolatum and inserted slowly into the rectum, and 1 mL of 8 % acetic acid was instilled once without excess pressure. Animals were then held briefly in position to prevent leakage and to ensure adequate mucosal contact, and were observed individually until recovery. Over the subsequent 20 days, general condition, motor activity, appetite, food and water intake, body-weight dynamics, stool consistency, the presence of diarrhoea, mucus or blood in the stool, and survival were monitored; deaths were recorded separately.

2.3. Tissue sampling and processing

At the end of the observation period, animals were withdrawn from the experiment in the morning on an empty stomach. Euthanasia was performed by decapitation under ether anaesthesia in accordance with bioethical requirements. After confirming the absence of pain reflexes, the abdominal cavity was opened along the midline and both kidneys were removed from the retroperitoneal space, cleared of perirenal fat and connective tissue, and examined macroscopically. Tissue fragments were fixed in 10 % neutral buffered formalin for 24 h, dehydrated through graded alcohols, cleared in orthoxylene and embedded in paraffin. Sections 4–5 μm thick were mounted on adhesive (poly-L-lysine/silane-coated) slides.

2.4. Immunohistochemistry

Immunohistochemical staining for Ki-67 and CD34 was performed to assess renal cell proliferation and the state of the microcirculation, respectively, using a standard avidin–biotin immunoperoxidase protocol. Sections were deparaffinised in xylene (three changes) and rehydrated through a descending ethanol series to distilled water. Heat-induced epitope retrieval was carried out in 0.01 M citrate buffer (pH 6.0) at sub-boiling temperature for 15–20 min, after which sections were allowed to cool at room temperature for ~20 min. Endogenous peroxidase activity was blocked with 3 % hydrogen peroxide for 10 min, followed by a protein block to reduce non-specific background. Sections were then incubated with the primary antibody (anti–Ki-67 or anti-CD34) for 60 min at room temperature. After buffer washing, a biotinylated secondary antibody was applied, followed by a streptavidin–horseradish-peroxidase (avidin–biotin) complex. The reaction was visualised with 3,3′-diaminobenzidine (DAB) chromogen for 5–10 min under microscopic control, and nuclei were counterstained with Mayer's haematoxylin; sections were then dehydrated, cleared and coverslipped. For each marker, a positive tissue control and a negative control (omission of the primary antibody) were processed in parallel. Antibody and protocol details are given in Table 2.

Antibody / target	Host & type	Clone	Source	Retrieval & dilution	Detection
Ki-67 (cell proliferation)	Rabbit monoclonal	SP6	Commercial supplier (see note)	Citrate pH 6.0, HIER; 1:100–1:200	Biotinylated 2nd Ab + streptavidin–peroxidase; DAB

Antibody / target	Host & type	Clone	Source	Retrieval & dilution	Detection
CD34 (endothelium / microvessels)	Rabbit polyclonal (rat-reactive)	Polyclonal	Commercial supplier (see note)	Citrate pH 6.0, HIER; 1:100–1:200	Biotinylated 2nd Ab + streptavidin–peroxidase; DAB

Table 2. Primary antibodies and immunohistochemical protocol. Note: retrieval, detection system and chromogen are as used in the study; antibody host, clone and working dilution follow standard immunohistochemical protocols for these markers and should be reconciled with the authors' laboratory records (exact supplier, catalogue number, lot and validated dilution) before submission. The CD34 antibody must be rat-reactive; the human clone QBEnd/10 is not recommended for rat tissue.

2.5. Evaluation of Ki-67

A positive Ki-67 reaction was defined as brown nuclear staining. Expression was assessed in the epithelium of proximal and distal tubules, interstitial cells, lymphocytes and histiocytes of the inflammatory infiltrate, fibroblasts, glomerular mesangial cells, capillary endothelium and podocytes. The proliferation index was expressed as the percentage of positively stained nuclei relative to all nuclei counted and graded semi-quantitatively as low (< 20 %), moderate (20–60 %) or high (> 60 %).

2.6. Evaluation of CD34 and microvessel density

A positive CD34 reaction was defined as brown membranous and cytoplasmic staining of endothelial cells. Glomerular capillaries, peritubular capillaries, interstitial microvessels, foci of neoangiogenesis in areas of inflammation and the capillary network within fibrotic zones were examined. For MVD, hotspot areas with the greatest number of CD34-positive structures were first identified at low magnification; CD34-positive microvessels were then counted in no fewer than five fields at ×200. Each discrete positively stained endothelial cell or cluster of endothelial cells, with or without a visible lumen, was counted as one microvessel (Weidner hotspot method) [17]. The relative CD34-positive area was additionally determined with QuPath 0.5.0 and expressed as a percentage of the total analysed tissue area.

2.7. Digital image analysis

Whole-field digital analysis was performed in QuPath 0.5.0. DAB-positive structures were segmented by colour deconvolution and threshold-based classification; background, lumina and artefacts were excluded from the analysed area. Ki-67 output was expressed as the percentage of positive nuclei and CD34 output as the percentage positive area.

2.8. Statistical analysis

Primary data were tabulated in Microsoft Excel and analysed in IBM SPSS Statistics 23. The distribution of quantitative variables was assessed with the Shapiro–Wilk test ($n < 50$) or the Kolmogorov–Smirnov test ($n > 50$), supplemented by skewness and kurtosis. Quantitative immunohistochemical indices are summarised descriptively as mean ± standard deviation (SD) with the standard error of the mean (SEM) and range; where per-animal data were available, normally distributed variables were compared between groups with the independent-samples Student t-test and non-normally distributed variables with the Mann–Whitney U-test. A two-sided $p < 0.05$ was considered statistically significant.

3. Results

3.1. Ki-67 proliferation index

In the control kidney, Ki-67 nuclear staining was rare and sporadic: isolated positive nuclei were found mainly in the epithelium of proximal and distal tubules and in occasional interstitial cells, consistent with the very low baseline proliferative activity reported for the normal kidney (~0.2–0.5 %) [9].

In the UC group the number of Ki-67-positive nuclei increased markedly. The strongest expression was seen in the tubular epithelium — particularly in zones of injury — in interstitial infiltrates (lymphocytes, histiocytes and fibroblasts) and in glomerular mesangial cells. Capillary endothelium and podocytes remained Ki-67-negative. Across the analysed representative fields ($n = 3$) the Ki-67 index ranged from 22.7 % to 59.7 %, with a mean of 35.4 % (SD 21.1; SEM 12.2), corresponding overall to a moderate level of expression (Table 3, Fig. 1, Fig. 3A).

Field	Structure with strongest signal	Ki-67+ nuclei (%)	Expression level
1	Tubular epithelium / interstitium	22.7	Moderate (+)
2	Tubular epithelium / interstitium	23.7	Moderate (+)
3	Injury-zone tubular epithelium / mesangium	59.7	Moderate–high (+)
Mean ± SD		35.4 ± 21.1	Moderate (+)

Table 3. Digital morphometric analysis of the renal Ki-67 proliferation index in the UC group (percentage of positive nuclei; n = 3 representative fields).

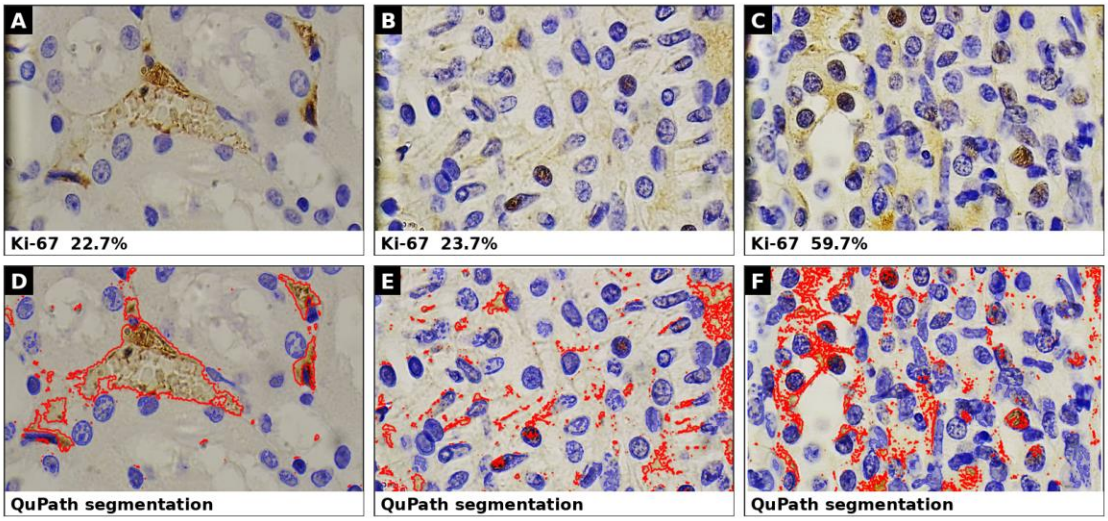

Figure 1. Ki-67 immunostaining of the kidney in experimental UC. (A–C) Representative fields with increasing proliferation index (22.7 %, 23.7 %, 59.7 %); brown nuclear DAB signal marks Ki-67-positive cells among haematoxylin-counterstained nuclei, predominantly in tubular epithelium, interstitial inflammatory cells and mesangium. (D–F) Corresponding QuPath 0.5.0 segmentation (red outlines = DAB-positive structures) used for automated quantification. Avidin–biotin immunoperoxidase, DAB, haematoxylin counterstain; original magnification ×400.

3.2. CD34 expression and microvessel density

In the control group, CD34 produced intense membranous staining of the endothelium of all vessels, and the microvessel density was 45.2 ± 2.1 vessels/mm². In the UC group, although endothelial staining was preserved, the microvascular architecture was clearly altered: focal neoangiogenesis was present in areas of inflammation, the peritubular capillary network was reduced (rarefied) in fibrotic areas, and glomerular CD34 expression was diminished in glomeruli showing mesangial expansion. Microvessel density fell to 32.8 vessels/mm², a reduction of 27.4 % relative to control (Fig. 3C). The relative CD34-positive area ranged from 55.6 % to 62.3 %, with a mean of 59.3 % (SD 3.4; SEM 2.0) (Table 4, Fig. 2, Fig. 3B).

Field	Compartment assessed	CD34+ area (%)	Expression level
4	Peritubular / interstitial microvessels	55.6	Moderate (+)
5	Peritubular / interstitial microvessels	60.0	Moderate (+)

Field	Compartment assessed	CD34+ area (%)	Expression level
6	Neoangiogenesis focus	62.3	High (+)
Mean ± SD		59.3 ± 3.4	Moderate (+)

Table 4. Digital morphometric analysis of the renal CD34-positive area in the UC group (n = 3 representative fields). Note: the value for Field 6 (62.3 %) and the mean (59.3 %) were corrected relative to the source dissertation, in which these two figures had been transposed.

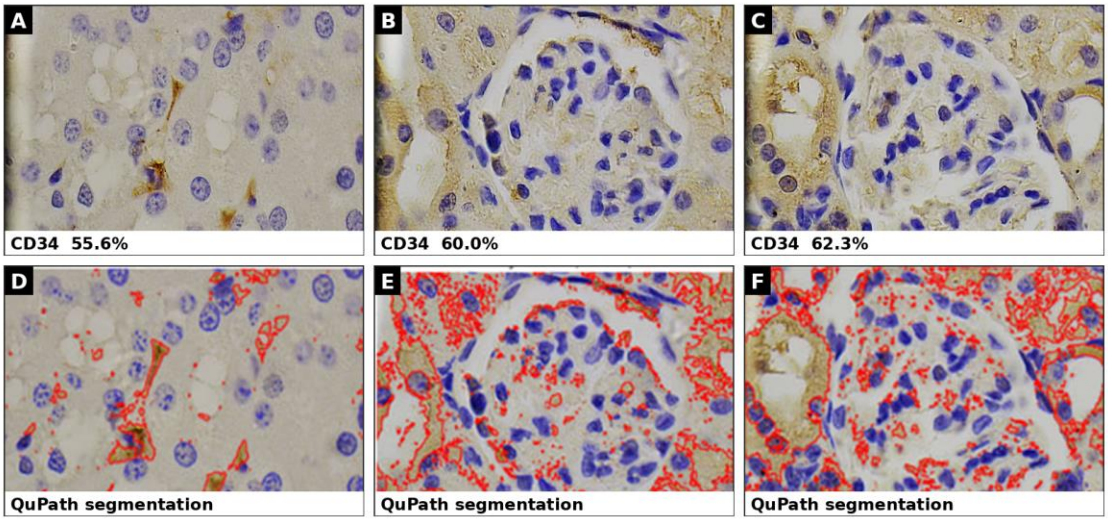

Figure 2. CD34 immunostaining of the kidney in experimental UC. (A–C) Representative fields (55.6 %, 60.0 %, 62.3 % positive area); brown membranous/cytoplasmic DAB signal marks endothelium of peritubular and interstitial microvessels and a focus of neoangiogenesis. (D–F) Corresponding QuPath 0.5.0 segmentation (red outlines = CD34-positive structures). Avidin–biotin immunoperoxidase, DAB, haematoxylin counterstain; original magnification ×400 (MVD counted at ×200).

3.3. Summary charts

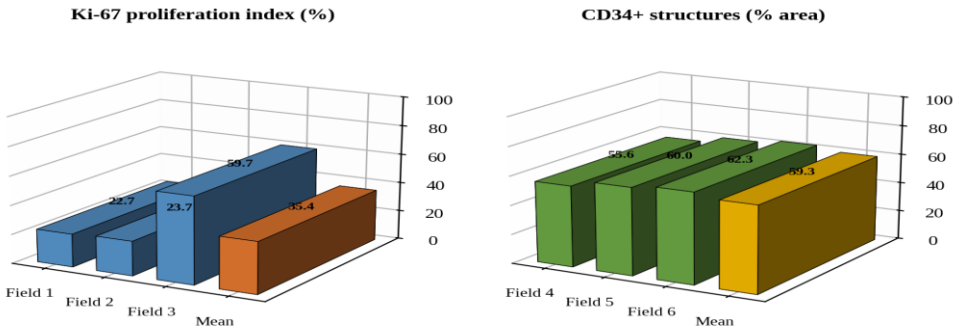

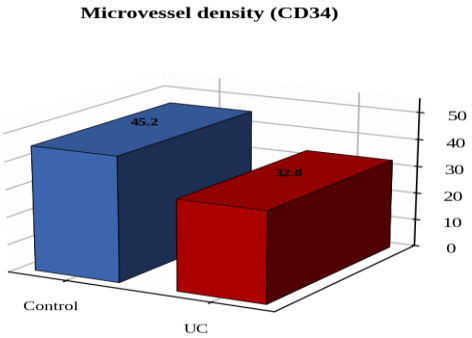

Figure 3. Quantitative immunohistochemical results. (A) Ki-67 proliferation index per field and mean. (B) CD34-positive area per field and mean. (C) CD34 microvessel density in control vs UC kidneys (−27.4 %). Editable three-dimensional versions of these charts are provided in the accompanying Excel workbook.

4. Discussion

The present study shows that experimentally induced UC is accompanied by two concurrent but opposite changes in the kidney: a marked rise in cellular proliferation (Ki-67) and a reduction in microvascular density (CD34). This proliferation–microcirculation dissociation provides a plausible tissue substrate for the progression of UC-associated renal injury towards interstitial fibrosis.

The increase in the Ki-67 index — from rare, sporadic nuclei in controls to a mean of 35.4 % in the UC group — was concentrated in the tubular epithelium of injury zones, in interstitial inflammatory cells and in glomerular mesangial cells. This distribution is consistent with the established biology of renal repair, in which surviving tubular epithelial cells de-differentiate and re-enter the cell cycle to restore the nephron after injury [10,11]; the very low baseline index in controls also matches reported proliferation indices for the normal kidney [9]. The prominent mesangial labelling parallels the mesangial hypercellularity of mesangioproliferative processes and echoes the use of Ki-67 to grade activity in IgA and lupus nephritis [11,12]. The absence of Ki-67 in endothelium and podocytes is in keeping with the largely post-mitotic character of these cells and indicates that the proliferative response is compartment-specific rather than global.

In parallel, CD34 immunostaining revealed a 27.4 % fall in microvessel density and rarefaction of the peritubular capillary network in fibrotic areas, together with reduced glomerular CD34 in glomeruli undergoing mesangial expansion. Peritubular capillary loss is a well-recognised driver of chronic tubulointerstitial injury: reduced capillary density promotes tissue hypoxia, which in turn stimulates fibrogenesis, and declining CD34-defined microvessel density has been repeatedly associated with the severity of renal interstitial fibrosis and with loss of renal function [13–16]. The focal neoangiogenesis observed here indicates that a compensatory angiogenic response is initiated but remains insufficient to restore the physiological capillary bed — an “angiogenic dysregulation” pattern also described after glomerular injury [13,14].

Taken together, these findings position the kidney as a genuine target organ of the systemic inflammatory burden of UC rather than an incidental bystander. The gut–kidney axis — encompassing systemic inflammation, circulating immune complexes, dysbiosis-derived metabolites and immune activation — offers a coherent mechanistic framework linking colonic ulceration to renal proliferation and microvascular remodelling [1,5,6]. The concurrence of heightened proliferation and capillary rarefaction is precisely the combination expected to favour maladaptive repair and fibrosis, consistent with the elevated long-term risk of CKD reported in IBD populations [1,4].

From a translational standpoint, Ki-67 and CD34 emerge as complementary quantitative read-outs: Ki-67 captures the proliferative activity of tubular, interstitial and mesangial compartments, while CD34 reports on endothelial integrity and peritubular capillary status. Assessed together — and ideally combined with morphometry and histochemistry of the extracellular matrix — they may serve as early indicators of UC-associated renal involvement and as objective end-points for evaluating nephroprotective or antifibrotic interventions in this model.

4.1. Limitations

The quantitative immunohistochemical read-outs reported here are based on representative high-power fields; per-animal quantification across the full cohorts, with formal between-group hypothesis testing, would further strengthen the

inferential statistics, and a data-entry template is provided in the accompanying workbook for this purpose. The control group was characterised qualitatively for both the nuclear (Ki-67) and area (CD34) indices, and a single time point was studied; a full time-course would clarify the temporal sequence of proliferation, rarefaction and fibrosis. These considerations do not affect the direction or internal consistency of the observed changes.

5. Conclusion

Experimentally induced ulcerative colitis causes a distinctive immunohistochemical signature in the rat kidney: a pronounced increase in Ki-67-defined proliferation of tubular, interstitial and mesangial cells, together with a reduction in CD34-defined microvessel density and peritubular capillary rarefaction that focal neoangiogenesis fails to compensate. This dissociation between enhanced proliferation and impaired microcirculation aggravates renal tissue injury and promotes the progression of fibrosis. Ki-67 and CD34 are therefore promising quantitative markers for the early detection, monitoring and mechanistic study of UC-associated nephropathy.

Declarations

Ethics approval. All animal procedures were approved by the Ethics Committee of the Bukhara State Medical Institute named after Abu Ali ibn Sino and conducted in accordance with institutional and international guidelines for the care and use of laboratory animals.

Author contributions. K. I. Kaymanova: conceptualisation, investigation, histological and immunohistochemical analysis, data curation, writing — original draft. B. A. Sanoev: supervision, methodology, validation, writing — review and editing. Both authors read and approved the final manuscript.

Funding. This research received no specific grant from any funding agency in the public, commercial or not-for-profit sectors.

Conflicts of interest. The authors declare that they have no competing interests.

Data availability. The data supporting the findings of this study are available from the corresponding author upon reasonable request.

References

1. Extraintestinal manifestations of inflammatory bowel disease: a focus on kidney complications. Int J Mol Sci. 2026;27(10):4614.
2. Renal and urological disorders associated with inflammatory bowel disease. Inflamm Bowel Dis. 2023;29(8):1306–1316.
3. Inflammatory bowel disease with chronic kidney disease and acute kidney injury. Am J Prev Med. 2023;65(6):1103–1112.
4. Risk of acute kidney injury in hospitalised patients with inflammatory bowel disease: a systematic review and meta-analysis. J Can Assoc Gastroenterol. 2026 (advance online).
5. Inflammatory bowel diseases and nephropathies: exploring the gut–kidney axis (narrative review). 2024.
6. Different renal manifestations associated with very early onset paediatric inflammatory bowel disease: case report and review of the literature. BMC Nephrol. 2021;22:146.
7. Suramin ameliorates acetic acid-induced acute colitis in rats through antioxidant and anti-inflammatory mechanisms. 2025.
8. Therapeutic potential of alpha-lipoic acid in a rat model of acetic acid-induced ulcerative colitis. Inflammopharmacology. 2025.
9. Nadasdy T, Laszik Z, Blick KE, Johnson LD, Silva FG. Proliferative activity of intrinsic cell populations in the normal human kidney. J Am Soc Nephrol. 1994;4(12):2032–2039.
10. Witzgall R, Brown D, Schwarz C, Bonventre JV. Localization of proliferating cell nuclear antigen, vimentin, c-fos and clusterin in the post-ischaemic kidney. J Clin Invest. 1994;93(5):2175–2188.
11. Cell-cycle behaviour of tubular epithelial cells and its dysregulation in renal repair and fibrosis (review). Front Cell Dev Biol. 2021;9:768.
12. Ki-67 proliferative index in immunoglobulin A nephropathy: a pilot study. 2022.
13. Ki-67 proliferation index in renal biopsy samples of patients with systemic lupus erythematosus and its correlation with clinical findings. 2013.
14. Identification of key genes related to peritubular capillary rarefaction in renal interstitial fibrosis, with CD34 immunohistochemistry. Sci Rep. 2023;13:19230.
15. Correlation between the renal resistive index, renal microvessel density (CD34) and interstitial fibrosis. 2024.
16. Choi YJ, Chakraborty S, Nguyen V, et al. Peritubular capillary loss is associated with chronic tubulointerstitial injury in human kidney: altered expression of vascular endothelial growth factor. Hum Pathol. 2000;31(12):1491–1497.
17. Weidner N. Current pathologic methods for measuring intratumoral microvessel density within breast carcinoma

and other solid tumors (hotspot method). Breast Cancer Res Treat. 1995;36(2):169–180.

18. Daehn IS, Duffield JS. The glomerular filtration barrier and endothelial–podocyte cross-talk in kidney disease. Nat Rev Nephrol. 2021;17:754–770.